

# MODELLING OF SUPPLY NETWORK DESIGN

Renata Majovská<sup>(a)</sup>, Petr Fiala<sup>(b)</sup>

<sup>(a)</sup> University of Finance and Administration, Prague

<sup>(b)</sup> University of Economics, Prague

<sup>(a)</sup> renata.majovska@mail.vsfs.cz, <sup>(b)</sup> pfiala@vse.cz

## ABSTRACT

The paper is dedicated to proposed modelling approach for supply networks. The original structure of network systems can be modelled as complex adaptive systems and use agent-oriented simulation to demonstrate origin. The structure is clarified by expert opinion with use of DEMATEL method. The suitability of supply networks can be measured by multiple objectives, such as economic, environmental, social, and others. Traditional concepts of optimality focus on valuation of already given systems. We propose to use a methodology for optimal system design. As a methodology of optimal system design can be employed De Novo Multi-objective Linear Programming for reshaping feasible sets in linear systems.

Keywords: supply networks, simulation, dynamics, DEMATEL, De Novo optimisation

## 1. INTRODUCTION

Supply network management has generated a substantial amount of interest both by managers and researchers (see Tayur et al. 2000). The design of supply networks plays an important role in supply network management. The suitability of supply networks can be measured by multiple objectives, such as economic, environmental, social, technological, and others. Supply network structure and behaviour is changing dynamically (Majovská and Fiala 2015, 2016).

Modelling of supply network design is not a simple matter, it is necessary to combine random elements with expert evaluation and parameter adjustments in dynamic changes. The aim of the paper is to propose such a procedure. The overall idea of the proposed procedure lies in the interconnected steps from simulating the design of the supply network, through expert assessment of the essential parts and links between them, to optimizing the design parameters, including the necessary resources to create a supply network within a specified budget. The contribution of this paper is the proposed three-stage procedure for multi-criteria design of supply networks:

- Generation of potential elements of supply network.
- Expert evaluation and simplification of the network structure.
- Continuous reconfiguration and reshaping of systems boundaries.

In this paper, the individual stages are modified and adapted to the needs of the design of supply networks and connected in an integrated approach. The first stage is based on a dynamic generation of potential elements of supply networks. Structure and behaviour dynamics of network systems can be modelled as complex adaptive systems and use agent-oriented simulation to demonstrate origin, perturbation effects, and sensitivity with regard to initial conditions. The model is based on a supply network as a system consisting of an environment in which firms create interactions based on simple rules of conduct to meet global demand (Fiala and Kuncová 2019).

The second stage is devoted to expert evaluation and simplification of the supply network structure. The DEMATEL (Decision Making Trial and Evaluation Laboratory) method (Gabus and Fontela 1972) is used for this stage.

The third stage is oriented on a continuous reconfiguration and reshaping of systems boundaries. Multi-objective supply network design is formulated and solved by De Novo approach. Traditional concepts of optimality focus on valuation of already given systems. New concept of designing optimal systems was proposed (Zeleny 2010). Multi-objective linear programming (MOLP) is a model of optimizing a given system by multiple objectives. As a methodology of optimal system design can be employed De Novo programming for reshaping feasible sets in linear systems. The paper presents approaches for solving the Multi-objective De Novo linear programming (MODNLP) problem for design of multi-objective supply networks. The approach is based on reformulation of MOLP problem by given prices of resources and the given budget. Searching for a better portfolio of resources leads to a continuous reconfiguration and reshaping of systems boundaries.

Technological innovations bring improvements to the desired objectives and the better utilization of available resources. These changes can lead to beyond tradeoff-free solutions. The de Novo approach was adapted for supply network design.

## 2. GENERATING SUPPLY NETWORKS

Supply network is defined as a system of clusters with:

- suppliers,
- manufacturers,
- distributors,
- retailers,
- customers,

where

- material,
- financial
- information,
- decision

flows connect participants in both directions (see Fiala 2005). A supply network is a complex and dynamic supply and demand network of agents, activities, resources, technology and information involved in moving a product or service from supplier to customer. Most supply networks are composed of independent units with individual preferences. Each unit will attempt to optimize his own preference. Behaviour that is locally efficient can be inefficient from a global point of view. An information asymmetry is a source of inefficiency in supply networks. The so-called bullwhip effect, describing growing variation upstream in a supply network, is probably the most famous demonstration of inefficiency and system dynamics in supply networks. Information sharing is a very important issue for coordinating actions of units in networks.

The dynamic generation of supply networks consists in generating potential network members and inter-relationships. To understand the growth and development of dynamics, it is necessary to monitor the time-dependent behaviour of the model. Simulation is a frequently used methodology for analysing the time-varying properties of a system. Agent-oriented simulation takes place in a system consisting of an environment in which agents (nodes) create interactions (edges) based on simple rules of conduct to meet global demand. Stochastic environmental parameters, describing market conditions and demand, a node-based decision-making scheme, so-called fitness functions modelling the strength of companies, all influence the dynamics of structure and behaviour of the developing supply network (Fiala and Kuncová 2019).

As new industries emerge, supply networks grow, creating new relationships between firms that cooperate to meet demand. New start-ups are involved in supply networks. Some companies significantly expanding capacity, while others weaken. An alternative scenario may be the fact that no companies become dominant and the market is relatively evenly distributed among participating firms. In a comprehensive adaptive supply network model, two aspects are considered:

- number of firms,
- size of firms.

The next step is to assess the significance of elements and relationships between them in the supply network.

## 3. DEMATEL METHOD

Expert evaluation and simplification of the supply network structure is done using the method DEMATEL. The DEMATEL method can be summarized in the following steps (Gabus and Fontela 1972):

### Step 1. Find the initial direct relation matrix.

Suppose we have  $m$  experts in this study and  $n$  elements to consider. Each expert is asked to indicate the degree to which he believes an element  $i$  affects an element  $j$ . These pairwise comparisons between any two elements are denoted by  $a_{ij}$  and are given an integer score ranging from 0, 1, 2, 3, and 4, representing:

- 0 no influence,
- 1 low influence,
- 2 medium influence,
- 3 high influence,
- 4 very high influence.

The scores by each expert will give us a  $(n, n)$  non-negative answer matrix  $\mathbf{X}^k = [x_{ij}^k]$ , with  $1 \leq k \leq m$ .

The diagonal elements of each answer matrix  $\mathbf{X}^k$  are all set to zero. We can then compute the  $(n, n)$  average matrix  $\mathbf{A}$  for all expert opinions by averaging the  $m$  experts' scores as follows:

$$a_{ij} = \frac{1}{m} \sum_{k=1}^m x_{ij}^k \quad (1)$$

The average matrix  $\mathbf{A}=[a_{ij}]$  is called the initial direct relation matrix. Matrix  $\mathbf{A}$  shows the initial direct effects that an element exerts on and receives from other elements. Furthermore, we can map out the causal effect between each pair of elements in a system by drawing an influence map. DEMATEL can convert the structural relations among the elements of a system into an intelligible map of the system.

### Step 2. Calculate the normalized initial direct-relation matrix.

The normalized initial direct-relation matrix  $\mathbf{D}$  is obtained by normalizing the initial direct-relation matrix  $\mathbf{A}$  in the following way:

Let

$$s = \max \left( \max_{1 \leq i \leq n} \sum_{j=1}^n a_{ij}, \max_{1 \leq j \leq n} \sum_{i=1}^n a_{ij} \right) \quad (2)$$

Then

$$\mathbf{D} = \frac{1}{s} \mathbf{A} \quad (3)$$

Since the sum of each row  $j$  of matrix  $\mathbf{A}$  represents the total direct effects that element  $i$  gives to the other

elements,  $\max_{1 \leq i \leq n} \sum_{j=1}^n a_{ij}$  represents the total direct effects

of the element with the most direct effects on others. Likewise, since the sum of each column  $i$  of matrix  $\mathbf{A}$  represents the total direct effects received by element  $i$ ,

$\max_{1 \leq j \leq n} \sum_{i=1}^n a_{ij}$  represents the total direct effects received of

the element that receives the most direct effects from others. The positive scalar  $s$  takes the lesser of the two as the upper bound, and the matrix  $\mathbf{D}$  is obtained by dividing each element of  $\mathbf{A}$  by the scalar  $s$ . Note that each element  $d_{ij}$  of matrix  $\mathbf{D}$  is between zero and one.

**Step 3.** Compute the total relation matrix.

A continuous decrease of the indirect effects of problems along the powers of matrix  $\mathbf{D}$  guarantees convergent solutions to the matrix inversion similar to an absorbing Markov chain matrix. Note that  $\lim_{k \rightarrow \infty} \mathbf{D}^k = \mathbf{0}$  and  $\lim_{k \rightarrow \infty} (\mathbf{I} + \mathbf{D} + \mathbf{D}^2 + \dots + \mathbf{D}^k) = (\mathbf{I} - \mathbf{D})^{-1}$ , where  $\mathbf{0}$  is the  $(n, n)$  null matrix and  $\mathbf{I}$  is the  $(n, n)$  identity matrix. The total relation matrix  $\mathbf{T}$  is an  $(n, n)$  matrix

$$\mathbf{T} = [t_{ij}] \quad i, j = 1, 2, \dots, n,$$

and is defined as follow:

$$\mathbf{T} = \mathbf{D} + \mathbf{D}^2 + \dots + \mathbf{D}^k = \mathbf{D}(\mathbf{I} + \mathbf{D} + \mathbf{D}^2 + \dots + \mathbf{D}^{k-1}) = \mathbf{D}(\mathbf{I} - \mathbf{D})^{-1}, \text{ as } k \rightarrow \infty. \quad (4)$$

Vectors  $\mathbf{r}$  and  $\mathbf{c}$  are defined representing the sum of rows and sum of columns of the total relation matrix  $\mathbf{T}$  as follows:

$$\mathbf{r} = (r_i) \quad (5)$$

where  $r_i$  be the sum of  $i$ -th row in matrix  $\mathbf{T}$ . Then  $r_i$  shows the total effects, both direct and indirect, given by element  $i$  to the other elements, and

$$\mathbf{c} = (c_j) \quad (6)$$

where  $c_j$  denotes the sum of  $j$ -th column in matrix  $\mathbf{T}$ . Then  $c_j$  shows the total effects, both direct and indirect, received by element  $j$  from the other elements.

Thus when  $j = i$ , the sum  $(r_i + c_i)$  gives an index representing the total effects both given and received by element  $i$ . In other words,  $(r_i + c_i)$  shows the degree of importance that element  $i$  plays in the system. In addition, the difference  $(r_i - c_i)$  shows the net effect that element  $i$  contributes to the system. When  $(r_i - c_i)$  is positive, element  $i$  is a net causer, and when  $(r_i - c_i)$  is negative, element  $i$  is a net receiver (Tzeng et al. 2007).

**Step 4.** Set a threshold value and obtain the impact-relations-map.

In order to explain the structural relation among the elements while keeping the complexity of the system to a manageable level, it is necessary to set a threshold value  $p$  to filter out some negligible effects in matrix  $\mathbf{T}$ . While each element of matrix  $\mathbf{T}$  provides information on how one element affects another, the decision-maker must set a threshold value in order to reduce the complexity of the structural relation model implicit in matrix  $\mathbf{T}$ . Only some elements, whose effect in matrix  $\mathbf{T}$  is greater than the threshold value, should be chosen and shown in an impact-relations-map (Tzeng et al. 2007).

**4. MULTI-OBJECTIVE SUPPLY NETWORKS**

In the next part, we formulate a multi-objective supply network design problem. The mathematical program determines the ideal locations for each facility and allocates the activity at each facility such that the multiple objectives are considered and the constraints of meeting the customer demand and the facility capacity are satisfied. The presented model of a supply network consists of 4 layers with  $m$  suppliers,  $S_1, S_2, \dots, S_m$ ,  $n$  potential producers,  $P_1, P_2, \dots, P_n$ ,  $p$  potential distributors,  $D_1, D_2, \dots, D_p$ , and  $r$  customers,  $C_1, C_2, \dots, C_r$ . The following notation is used:

$a_i$  = annual supply capacity of supplier  $i$ ,  $b_j$  = annual potential capacity of producer  $j$ ,  $w_k$  = annual potential capacity of distributor  $k$ ,  $d_l$  = annual demand - customer  $l$ ,

$f_j^P$  = fixed cost of potential producer  $j$ ,  $f_k^D$  = fixed cost of potential distributor  $k$ ,

$c_{ij}^S$  = unit transportation cost from  $S_i$  to  $P_j$ ,  $c_{jk}^P$  = unit transportation cost from  $P_j$  to  $D_k$ ,

$c_{kl}^D$  = unit transportation cost from  $D_k$  to  $C_l$ ,  $e_{ij}^S$  = unit pollution from  $S_i$  to  $P_j$ ,

$e_{jk}^P$  = unit pollution from  $P_j$  to  $D_k$ ,  $e_{kl}^D$  = unit environmental pollution from  $D_k$  to  $C_l$ ,

$x_{ij}^S$  = number of units transported from  $S_i$  to  $P_j$ ,  $x_{jk}^P$  = number of units transported from  $P_j$  to  $D_k$ ,  $x_{kl}^D$  = number of units transported from  $D_k$  to  $C_l$ ,

$y_j^P$  = bivalent variable for build-up of fixed capacity of producer  $j$ ,

$y_k^D$  = bivalent variable for build-up of fixed capacity of distributor  $k$ .

Using the above notations the problem can be formulated as follows:

The model has two objectives. The first one expresses minimizing of total costs. The second one expresses minimizing of total environmental pollution.

Min

$$z_1 = \sum_{j=1}^n f_j^P y_j^P + \sum_{k=1}^p f_k^D y_k^D + \sum_{i=1}^m \sum_{j=1}^n c_{ij}^S x_{ij}^S + \sum_{j=1}^n \sum_{k=1}^p c_{jk}^P x_{jk}^P + \sum_{k=1}^p \sum_{l=1}^r c_{kl}^D x_{kl}^D$$

Min

$$z_2 = \sum_{i=1}^m \sum_{j=1}^n e_{ij}^S x_{ij}^S + \sum_{j=1}^n \sum_{k=1}^p e_{jk}^P x_{jk}^P + \sum_{k=1}^p \sum_{l=1}^r e_{kl}^D x_{kl}^D$$

Subject to the following constraints:

the amount sent from the supplier to producers cannot exceed the capacity

$$\sum_{j=1}^n x_{ij} \leq a_i, \quad i = 1, 2, \dots, m,$$

the amount produced by the producer cannot exceed the producer capacity

$$\sum_{k=1}^p x_{jk} \leq b_j y_j, \quad j = 1, 2, \dots, n,$$

the amount shipped from the distributor should not exceed the distributor capacity

$$\sum_{l=1}^r x_{kl} \leq w_k y_k, \quad k = 1, 2, \dots, p,$$

the amount shipped to the customer must equal the customer demand

$$\sum_{k=1}^p x_{kl} = d_l, \quad l = 1, 2, \dots, r,$$

the amount shipped out of producers cannot exceed units received from suppliers

$$\sum_{i=1}^m x_{ij} - \sum_{k=1}^p x_{jk} \geq 0, \quad j = 1, 2, \dots, n,$$

the amount shipped out of distributors cannot exceed quantity received from producers

$$\sum_{j=1}^n x_{jk} - \sum_{l=1}^r x_{kl} \geq 0, \quad k = 1, 2, \dots, p,$$

binary and non-negativity constraints

$$y_j, y_k \in \{0, 1\},$$

$$x_{ij}, x_{jk}, x_{kl} \geq 0, \quad i=1, 2, \dots, m, \quad j=1, 2, \dots, n, \quad k=1, 2, \dots, p, \quad l=1, 2, \dots, r.$$

The formulated model is a multi-objective linear programming problem (MOLP). The problem can be solved by some MOLP methods.

## 5. OPTIMIZING GIVEN SYSTEMS

Multi-objective linear programming (MOLP) is a model of optimizing a given system by multiple objectives. In MOLP problems it is usually impossible to optimize all objectives together in a given system. Trade-off means that one cannot increase the level of satisfaction for an objective without decreasing this for another objective. Multi-objective linear programming (MOLP) problem can be described as follows

$$\begin{aligned} \text{“Max” } & z = Cx \\ \text{s.t. } & Ax \leq b, \quad x \geq 0 \end{aligned} \quad (7)$$

where  $C$  is a  $(k, n)$  – matrix of objective coefficients,  $A$  is a  $(m, n)$  – matrix of structural coefficients,  $b$  is an  $m$ -vector of known resource restrictions,  $x$  is an  $n$ -vector of decision variables. In MOLP problems it is usually impossible to optimize all objectives in a given system. For multi-objective programming problems the concept of non-dominated solutions is used (see for example

Steuer 1986). A compromise solution is selected from the set of non-dominated solutions. There are proposed many methods. Most of the methods are based on trade-offs. The next part is devoted to the trade-off free approach.

## 6. DESIGNING OPTIMAL SYSTEMS

Multi-objective De Novo linear programming (MODNLP) is a problem for designing an optimal system by reshaping the feasible set. By given prices of resources and the given budget the MOLP problem (7) is reformulated in the MODNLP problem (8)

$$\begin{aligned} \text{“Max” } & z = Cx \\ \text{s.t. } & Ax - b \leq 0, \quad pb \leq B, \quad x \geq 0 \end{aligned} \quad (8)$$

where  $b$  is an  $m$ -vector of unknown resource restrictions,  $p$  is an  $m$ -vector of resource prices, and  $B$  is the given total available budget.

From (8) follows  $pAx \leq pb \leq B$ .

Defining an  $n$ -vector of unit costs  $v = pA$  we can rewrite the problem (8) as

$$\begin{aligned} \text{“Max” } & z = Cx \\ \text{s.t. } & vx \leq B, \quad x \geq 0 \end{aligned} \quad (9)$$

Solving single objective problems

$$\begin{aligned} \text{Max } & z^i = c^i x, \quad i = 1, 2, \dots, k \\ \text{s.t. } & vx \leq B, \quad x \geq 0 \end{aligned} \quad (10)$$

$z^*$  is a  $k$  – vector of objective values for the ideal system with respect to  $B$ .

The problems (10) are continuous “knapsack” problems, the solutions are

$$x_j^i = \begin{cases} 0, & j \neq j_i \\ B/v_j, & j = j_i \end{cases},$$

where  $j_i \in \{j \in (1, \dots, n) \mid \max_j (c_j^i / v_j)\}$ .

The meta-optimum problem can be formulated as follows

$$\begin{aligned} \text{Min } & f = vx \\ \text{s.t. } & Cx \geq z^*, \quad x \geq 0 \end{aligned} \quad (11)$$

Solving the problem (11) provides solution:  $x^*$ ,  $B^* = vx^*$ ,  $b^* = Ax^*$ .

The value  $B^*$  identifies the minimum budget to achieve  $z^*$  through solutions  $x^*$  and  $b^*$ .

The given budget level  $B \leq B^*$ . The optimum–path ratio for achieving the best performance for a given budget  $B$  is defined as

$$r_1 = \frac{B}{B^*}$$

The optimum-path ratio provides an effective and fast tool for the efficient optimal redesign of large-scale linear systems. Optimal system design for the budget  $B$ :

$$x = r_1 x^*, b = r_1 b^*, z = r_1 z^*.$$

## 7. DE NOVO APPROACH FOR MULTI-OBJECTIVE SUPPLY NETWORKS

The De Novo approach can be useful in the design of the multi-objective supply network. Only a partial relaxation of constraints is adopted. Producer and distributor capacities are relaxed. Unit costs for capacity build-up are computed:

$$p_j^P = \frac{f_j^P}{b_j} = \text{cost of unit capacity of potential producer } j,$$

producer  $j$ ,

$$p_k^D = \frac{f_k^D}{w_k} = \text{cost of unit capacity of potential distributor } k.$$

distributor  $k$ .

Variables for build-up capacities are introduced:

$$u_j^P = \text{variable for flexible capacity of producer } j,$$

$$u_k^D = \text{variable for flexible capacity of producer } k.$$

The constraints for non-exceeding producer and distributor fixed capacities are replaced by the flexible capacity constraints and the budget constraint:

$$\sum_{k=1}^p x_{jk} - u_j^P \leq 0, j = 1, 2, \dots, n,$$

$$\sum_{l=1}^r x_{kl} - u_k^D \leq 0, k = 1, 2, \dots, p,$$

$$\sum_{j=1}^n p_j^P u_j^P + \sum_{k=1}^p p_k^D u_k^D \leq B.$$

The multi-objective optimization can be then seen as a dynamic process. Technological innovations bring improvements to the desired objectives and the better utilization of available resources. The technological innovation matrix  $T = (t_{ij})$  is introduced. The elements in the structural matrix  $A$  should be reduced by a technological progress. The problem (8) is reformulated in to the innovation MODNLP problem (12)

$$\begin{aligned} \text{“Max”} &= Cx \\ \text{s.t. } TAx - b &\leq 0, pb \leq B, x \geq 0 \end{aligned} \quad (12)$$

De Novo approach provides a better solution in multiple objectives and also with lower budget because of flexible capacity constraints. The capacity of supply network members has been optimized with regard to flows in the supply network and to budget.

## 8. CASE STUDY

We tested the De Novo approach on a case study. A supply network is proposed with 3 potential suppliers, 3 potential manufacturers, 3 potential distributors, 3 customers. The network is evaluated according to 2 criteria, the first criterion is aimed at minimizing total costs and the second one at minimizing overall environmental pollution. Inputs for the model are as follows:

Capacities  $a_i = 100, i = 1, 2, 3; b_j = 100, j = 1, 2, 3;$   
 $w_k = 100, k = 1, 2, 3; d_l = 50, l = 1, 2, 3.$

Fixed costs  $f_1^P = 110, f_2^P = 100, f_3^P = 120, f_1^D = 120,$   
 $f_2^D = 110, f_3^D = 150.$

Unit transport costs and unit pollution are shown in the Table 1 and Table 2.

Table 1: Unit transport costs

$c_{ij}^S$	1	2	3	$c_{jk}^P$	1	2	3	$c_{kl}^D$	1	2	3
1	5	10	6	1	7	5	9	1	8	3	10
2	8	9	7	2	6	8	4	2	6	5	4
3	3	6	8	3	5	7	9	3	7	3	5

Table 2: Unit pollution

$e_{ij}^S$	1	2	3	$e_{jk}^P$	1	2	3	$e_{kl}^D$	1	2	3
1	4	3	8	1	8	7	9	1	8	6	2
2	8	9	2	2	6	8	4	2	8	9	8
3	7	6	8	3	4	7	9	3	5	3	5

This model was solved by different approaches. The first two approaches minimize each criterion separately. The compromise solution is calculated by the traditional STEM interactive approach for multi-criterion tasks and the De Novo approach was used. The following are non-zero values of the variables that express the number of units of product shipped between each supply network layer. These values are given for each problem-solving approach.

Min  $z_1$ :  $x_{13}^S = 50, x_{31}^S = 100, x_{12}^P = 100, x_{31}^P = 50, x_{12}^D = 50, x_{21}^D = 50, x_{23}^D = 50.$

Min  $z_2$ :  $x_{12}^S = 100, x_{23}^S = 50, x_{23}^P = 100, x_{31}^P = 50, x_{13}^D = 50, x_{31}^D = 50, x_{32}^D = 50.$

STEM:  $x_{11}^S = 58.13, x_{23}^S = 91.87, x_{12}^P = 58.13, x_{31}^P = 91.87, x_{12}^D = 46.87, x_{13}^D = 45, x_{21}^D = 50, x_{22}^D = 3.12, x_{23}^D = 50.$

De Novo:  $x_{23}^S = 62.86, x_{32}^S = 87.14, x_{21}^P = 10, x_{23}^P = 77.14, x_{31}^P = 62.86, x_{12}^D = 50, x_{13}^D = 22.86, x_{31}^D = 50, x_{33}^D = 27.14.$

The criteria values  $z_1$  a  $z_2$  and the budget  $B$  are compared according to these solutions. De Novo solution is better in all values than the STEM solution. De Novo approach provides better solutions on both criteria and also with a lower budget due to flexible capacity constraints. The capacity of supply network members have been optimized for flows in the supply network and budget. The comparison of results are shown in Table 3.

Table 3: Comparison of solution results

	Min $z_1$	Min $z_2$	STEM	De Novo
$z_1$	2460	3490	3070	3000
$z_2$	3100	1800	2030	2000
$B$	460	490	460	365.71

## 9. CONCLUSIONS

The proposed methodology of supply network design modelling consists of three stages. In the first stage, the network system of potential members and their interconnections is simulated. The second stage is

devoted to expert evaluation of the proposed network system by the DEMATEL method. In the third stage, De Novo approach was applied for multi-objective supply network design problem and provides better solution than traditional approaches applied on fixed constraints. The design problem was formulated as MOLP problem. The economic and environmental objectives were used in the model but multiple objectives can be used in general. Technological innovations bring improvements to the desired objectives and the better utilization of available resources. These changes can lead to beyond tradeoff-free solutions. The combination of these three stages and their repetition over time provides an efficient and flexible tool for modeling supply network design. The approach can be enriched with other tools such as game theory (Fiala 2016).

#### ACKNOWLEDGMENTS

The paper is a result of institutional research project no. 7429/2018/08 "Analysis of ICT startups" supported by University of Finance and Administration, Prague and Grant No. IGA F4/66/2019, Faculty of Informatics and Statistics, University of Economics, Prague.

#### REFERENCES

- Fiala, P., 2005. Information sharing in supply chains. *Omega*, 33 (4), 419-423.
- Fiala, P., 2016. Profit allocation games in supply chains. *Central European Journal of Operations Research*, 24 (2), 267-281.
- Fiala, P., Kuncová, M., 2019. Simulation model of supply networks development. *Proceedings of International Conference on Modelling and Applied Simulation*. September 18-20, Lisbon (Portugal).
- Mathematical Methods in Economics*, pp. 86–91. September 12-14, Jindřichův Hradec (Czech Republic).
- Fiala, P., Majovská, R., 2018. Modeling of supply network coordination. *Proceedings of Mathematical Methods in Economics*, pp. 86–91. September 12-14, Jindřichův Hradec (Czech Republic).
- Fiala, P., Majovská, R., 2018. Design of Supply Networks by De Novo Method (in Czech). *Trendy v podnikání*, 8 (3), 32–38.
- Gabus, A., Fontela, E., 1972. World problems, an invitation to further thought within the framework of DEMATEL. Geneva: Battelle Geneva Research Centre.
- Majovská, R., Fiala, P., 2015. Dynamic analysis of multi-criteria network systems. *Proceedings of Mathematical Methods in Economics*, pp. 484–490. September 9-11, Cheb (Czech Republic).
- Majovská, R., Fiala, P., 2016. Modelling of dynamic network systems. *Proceedings of the Quantitative Methods in Economics*, pp. 236–240. May 25-27, Vrátna (Slovak Republic).
- Steuer, R. E. 1986. *Multiple Criteria Optimization: Theory, Computation and Application*. New York: Wiley.
- Tayur, S., Ganeshan, R., Magazine, M., 2000. *Quantitative models for supply chain management*. Boston: Kluwer.
- Tzeng, G. H., Chiang, C. H., Li, C. W., 2007. Evaluating intertwined effects in e-learning programs: A novel hybrid MCDM model based on factor analysis and DEMATEL. *Expert Systems with Applications* 32, 1028–1044.
- Zelený, M., 2010. Multiobjective Optimization, Systems Design and De Novo Programming. In: C. Zopounidis, P. M. Pardalos, ed. *Handbook of Multicriteria Analysis*. Berlin: Springer, 243-262.

#### AUTHORS BIOGRAPHY

**Renata Majovská:** She earned her degree in Mathematics and Physics at the Technical University in Ostrava, Czech Republic. She gained her PhD. at the Constantine the Philosopher University in Nitra, Slovakia in 2008. She is the Assistant Professor at the University of Finance and Administration in Prague, Czech Republic. She is a member of the Czech Society of Operational Research. Dr. Majovská has participated in the solving of several grants and is a co-author of several books and author of many scientific and conference papers in modelling of production systems, supply chain management, multi-criteria and group decision making. She has prepared many electronic university textbooks.

**Petr Fiala:** He holds the Full Professor degree from the University of Economics in Prague, Czech Republic, where he currently works as the Deputy Head of the Department of Econometrics. He is a member of other Czech universities. Professor Fiala is graduated from the University of Economics in Prague, in 1974, Charles University, Prague, in 1981, and Rochester Institute of Technology, USA, in 1996. His current research interests include modelling of production systems, supply chain management, project management, multi-criteria and group decision making. He is a member of professional societies for Operations Research and Multiple Criteria Decision Making and the Czech Republic representative in EURO (The Association of European Operational Research Societies). He has made research visits to many countries. He is the author of books, lecture notes, papers, and reports in quantitative models and methods in management and economics.

# OPTIMAL HYBRID DRIVE SYSTEM ARCHITECTURE EXPLORATION CONSIDERING PERFORMANCE INDEX OF 48V MILD HEV

Yonghyeok Ji<sup>(a)</sup>, Taeho Park<sup>(b), (c)</sup>, Hyeongcheol Lee<sup>\*(d)</sup>

<sup>(a),(b)</sup>Department of Electrical Engineering, Hanyang University, 222, Wangsimni-ro, Seongdong-gu, Seoul 133-791, Korea

<sup>(c)</sup>Green Car Power System R&D Division, Korea Automotive Technology Institute, 303 Pungse-ro, Pungse-myeon, Dongnam-gu, Cheonan-si, Chungnam 31214, Korea

<sup>(d)</sup>Department of Electrical and Biomedical Engineering, Hanyang University, 222, Wangsimni-ro, Seongdong-gu, Seoul 133-791, Korea

<sup>(a)</sup>[young0839@hanyang.ac.kr](mailto:young0839@hanyang.ac.kr), <sup>(b), (c)</sup>[koreapow@hanyang.ac.kr](mailto:koreapow@hanyang.ac.kr), <sup>(d)</sup>[hcleee@hanyang.ac.kr](mailto:hcleee@hanyang.ac.kr)

\*Corresponding Author [hcleee@hanyang.ac.kr](mailto:hcleee@hanyang.ac.kr)

## ABSTRACT

The 48V hybrid system has mostly adopted parallel hybrid system architecture. In the parallel hybrid system, various architecture can be derived depending on the location of the motor. In this paper, we explored a hybrid system architecture considering one or two motors and 48V electric supercharger and derived the optimal architecture by comparing the performance of each architecture. Performance of the hybrid system is mostly evaluated as fuel economy. However, since the hybrid system has increasingly been applied to various types of vehicles with different purpose of the operation, another performance index for evaluating a hybrid system is needed. Therefore, in this paper, we introduced an additional performance index to evaluate the hybrid electric drive system and used it to derive the optimal architecture of the hybrid electric drive system. We used *Dynamic programming (DP)* to evaluate each architecture and *DP* simulation was performed in the Matlab environment.

Keywords: 48V mild hybrid system, HEV architecture, *Dynamic programming*, Performance index

## 1. INTRODUCTION

As fuel economy and emission gas regulations are strengthened globally, environmentally friendly vehicles of various types (BEV, FCEV, (P)HEV, etc.) are being introduced to the market. However, due to the problem of the high-cost electric drive system or charging infrastructure, it is still difficult for vehicles to replace the demand for existing internal combustion engine vehicles. According to this trend, a mild hybrid system based on a 48V power supply has recently attracted attention as a new alternative and many kinds of research about 48V mild hybrid system are being conducted. (Malte Kuypers 2014; Mark Schudeleit and Christian Sieg 2015; Anthony Rick and Brain Sisk 2015; Andreas Baumgardt and Dieter Gerling 2015a,b;

Anthony Rick and Brain Sisk 2015; Zifan Liu and Andrej Ivanco 2016; Junyong Park and Taeho Park 2017)

There are various hybrid drive system architectures according to the arrangement of the hybrid drive system component such as the engine, the motor, and the gearbox. 48V hybrid drive systems adopt parallel hybrid architecture mostly, and parallel hybrid architectures are generally divided into P0~P4 according to the location of the motor (Figure 1). And many studies have been done on the CO<sub>2</sub> reduction effect and cost efficiency for each configuration. (Dr. Ing. Olivier COPPIN 2016; Ran Bao and Victor Avila 2017; Thomas Eckenfels and Florian Kolb 2018)

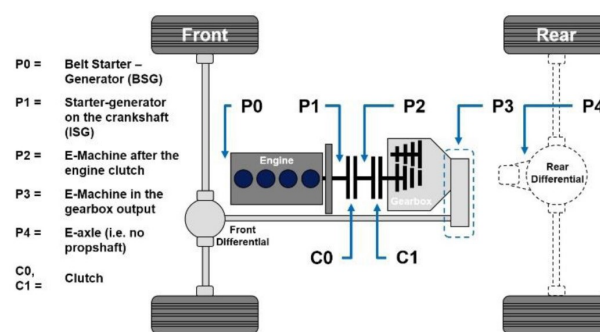


Figure 1: P0~P4 Architecture

However recently, there are the cases composing a 48V hybrid system including not only one motor but also two motor or a 48V electric supercharger, and there is still a lack of research on which architecture is optimal when these components are considered in 48V hybrid system configuration.

The performance of a hybrid system is evaluated with fuel economy mostly. But a hybrid system has been being adapted to various vehicle segments, and since a consumer's expectation is different by vehicle segments, it is needed that evaluating vehicle with performance

other than fuel economy. As related research, Kapadia (2017) compared P2 parallel hybrid architecture and input split hybrid architecture in terms of not only fuel economy but also drivability, launch, power, towing performance and packaging, etc.

Therefore, in this paper, we derived an optimal 48V hybrid system architecture according to fuel economy and performance index when one or two 48V motor and 48V electric supercharger are considered. To do this, we explored 48V hybrid system architecture manually when one or two 48V motors, 48V electric supercharger are considered, and we derived an optimal architecture through *Dynamic programming*. In this case, the cost function of *Dynamic programming* was modified to derive optimal architecture for fuel economy and performance index. Here, the performance index is the index which can evaluate hybrid system performance other than fuel economy, and in this paper, we defined an electric auxiliary load assist ability and drive power reserve as a performance index.

## 2. EXPLORATION TARGET HYBRID DRIVE ARCHITECTURE

When considering one motor, a 48V hybrid system architecture which can be derived is like Figure 1. In this case, since P0 and P1 architectures have lower fuel economy than P2, P3, and P4 generally, we select P2, P3, and P4 architecture as exploration target hybrid drive architecture having one motor.

And we select the exploration target hybrid drive architecture having two motors like Figure 2. In the figure, the P0D architecture is the architecture that can operate mechanical auxiliary load (ex. water pump, air-conditioner compressor) independently by separating the mechanical auxiliary load from the engine according to the situation. And the motor location is the same as P0 architecture. Since P0D has little higher fuel economy than P0 generally, which is not suggested in this paper, we select P0D architecture instead of P0 architecture for exploration.

Therefore, we select 10 exploration target 48V hybrid drive architecture like below according to motor location and the number of motors.

1. Using one motor: P2, P3, P4
2. Using two motor: P0D+P2, P0D+P3, P0D+P4  
P1+P2, P1+P3, P1+P4  
P2+P4

But, above 10 architecture doesn't consider a 48V electric supercharger. Therefore finally, we select a total 20 exploration target 48V hybrid drive system architecture by adding 10 architecture having a 48V electric supercharger.

Table 1 below is the specification of the hybrid drive system main components. As we can see in the table, the motor power when using two motors is half of the power when using one motor.

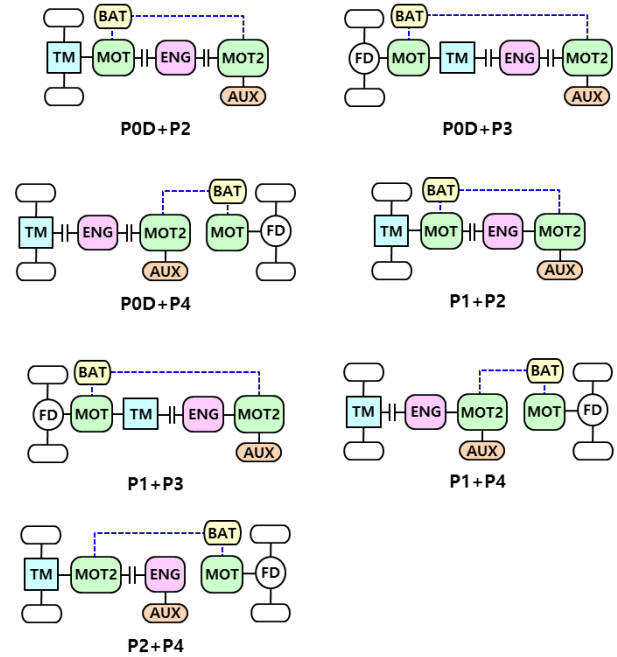


Figure 2: 48V Hybrid Drive System Architecture with Two Motor

Table 1: Specification of Vehicle Component

Component	Specification
Engine	1500 [cc] Gasoline Engine
Motor	10 [kW] PMSM (when using one motor)
	5 [kW] PMSM (when using two motor)
Electric Supercharger	5 [kW] PMSM
Battery	48 [V] / 20 [Ah] Lithium-Ion

## 3. MODEL FOR DYNAMIC PROGRAMMING

We used *Dynamic Programming (DP)* to compare each exploration target hybrid drive system architecture. *DP* is a method of global optimization strategies that find optimal solutions to optimal control problems based on Bellman's principle of optimality. For the hybrid drive system, *DP* is mainly used to analyze the optimal fuel economy results by investigating all possible paths of the vehicle system in a given driving cycle in advance. Therefore, the *DP* results for any hybrid system architecture can be said to be the optimal performance of the architecture. So, we carry out *DP* simulation about each exploration target hybrid drive architecture and derives optimal architecture by comparing *DP* results.

### 3.1. Dynamic programming with dpm.m function

In this paper, we use Matlab function *dpm.m* for *DP*. *dpm.m* is a *DP* algorithm introduced by Olle Sundström and Lino Guzzella (2009) to solve the general optimization problem. To solve the optimal control problem using the *dpm.m* function, the user must define the *Main.m* function and the *Model function.m* function. The *Main.m* function sets the range and grid of control



input, state for  $DP$  and executes  $dpm.m$ . Model function.m uses the given inputs to calculate the cost and the state of the next step and returns these values to  $dpm.m$ . In this paper, the model function is the vehicle model that calculates the fuel consumption and the SOC variation according to the power distribution ratio, the electric supercharger speed, and transmission gear stage.

### 3.2. Main.m function setting

As mentioned in Section 3.1, we need the Main.m function and the Model function.m to use  $dpm.m$ . This section introduces the settings for the Main.m function. First, we define the control input as below.

1.  $u_1$  : Power distribution ratio for the first motor
2.  $u_2$  : 48V electric supercharger speed
3.  $u_3$  : Gear shift command
4.  $u_4$  : Decoupler on/off command
5.  $u_5$  : Power distribution ratio for the second motor

The decoupler on/off command  $u_4$  is applied to the architecture considering P0D motor, the Power distribution ratio for the second motor  $u_5$  is applied to the architecture considering two motors. The activated control inputs according to architecture is like Table 2.

**Table 2: Control Input Setting according to Hybrid Drive System Architecture (O: Use, -: Not use)**

Architecture	$u_1$	$u_2$	$u_3$	$u_4$	$u_5$
P2	O	O	O	-	-
P3	O	O	O	-	-
P4	O	O	O	-	-
P0D+P2	O	O	O	O	O
P0D+P3	O	O	O	O	O
P0D+P4	O	O	O	O	O
P1+P2	O	O	O	-	O
P1+P3	O	O	O	-	O
P1+P4	O	O	O	-	O
P2+P4	O	O	O	-	O

The mathematical equation of each control input is defined as follows.

First,  $u_1$  and  $u_5$  are defined like Table 3. In the equations below,  $\gamma_{ply}, \gamma_{TM}$  is the gear ratio of engine pulley and transmission respectively,  $T_{m,i}$  is the motor torque,  $T_{tot,i}$  is the vehicle total desired torque ( $i=2$  for P2, 3 for P3, 0D3 for P0D+P3 etc.). And  $T_{tot,f,j}$  is the value of vehicle total desired torque minus P4 motor torque in the architecture having P4 motor. ( $j=0D4, 14, 24$ ). As we can see in the table,  $u_1$  determines the

power distribution of motor which is located relatively far from the engine,  $u_5$  determines the power distribution of the motor which is located relatively close to the engine.

**Table 3: Equation of Control Input  $u_1, u_5$**

Architecture	$u_1$	$u_5$
P2	$T_{m,2}/T_{tot,2}$	-
P3	$T_{m,3}/T_{tot,3}$	-
P4	$T_{m,4}/T_{tot,4}$	-
P0D+P2	$T_{m,2}/T_{tot,0D2}$	$\gamma_{ply} T_{m,0D}/T_{tot,0D2}$
P0D+P3	$T_{m,3}/T_{tot,0D3}$	$\gamma_{TM} \gamma_{ply} T_{m,0D}/T_{tot,0D3}$
P0D+P4	$T_{m,4}/T_{tot,0D4}$	$\gamma_{TM} \gamma_{ply} T_{m,0D}/T_{tot,f,0D4}$
P1+P2	$T_{m,2}/T_{tot,12}$	$T_{m,1}/T_{tot,12}$
P1+P3	$T_{m,3}/T_{tot,13}$	$\gamma_{TM} T_{m,1}/T_{tot,13}$
P1+P4	$T_{m,4}/T_{tot,14}$	$\gamma_{TM} T_{m,1}/T_{tot,f,14}$
P2+P4	$T_{m,4}/T_{tot,24}$	$\gamma_{TM} T_{m,2}/T_{tot,f,24}$

$u_3, u_4$  are defined like Equation (1), (2) respectively.

In Equation (2), Decoupler open means the case that mechanical auxiliary load is separated from an engine, and Decoupler close means the case that mechanical auxiliary load is connected to an engine.

$$u_3 = \begin{cases} 1 & (\text{Upshift}) \\ 0 & (\text{No shift}) \\ -1 & (\text{Downshift}) \end{cases} \quad (1)$$

$$u_4 = \begin{cases} 1 & (\text{Decoupler open}) \\ 0 & (\text{Decoupler close}) \end{cases} \quad (2)$$

The range and grid of each control input are like Table 4.

**Table 4: Range and Grid of Control Input**

Control Input	Range	Grid points	Unit
$u_1$	-1 ~ 1	21	-
$u_2$	0 ~ 143,000	21	RPM
$u_3$	-1 ~ 1	3	-
$u_4$	0 ~ 1	2	-
$u_5$	-1 ~ 1	21	-

We define states as 48V battery SOC, an engine on/off state, and gear stage of transmission. The range and grid of each state are like Table 5.

**Table 5: Range and Grid of State**

Control Input	Range	Grid points
SOC	0.3 ~ 0.9	21
Engine On/Off	0 ~ 1	2
Gear Stage	1 ~ 6	6

### 3.3. Model function.m setting

This section introduces the Model function.m for DP. As mentioned above, the model function in this paper is a vehicle model, and the model used in this study is basically the same as the model which was used in the study last year (Ji Y. and Park J. 2018). Therefore, in this paper, we only describe the values which are defined differently from the last year's study depending on the exploration target hybrid system architecture. The values that are defined differently by architecture are vehicle total desired torque, motor torque, cost function.

#### 3.3.1. Total desired torque determination

The vehicle model used in last year's study is P0 architecture. So, the vehicle total desired torque is calculated at the engine crankshaft. In this paper, we define the calculation location of vehicle total desired torque according to architecture, for the convenience of calculation, like Figure 3.

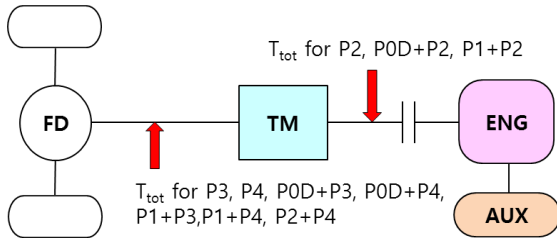


**Figure 3: Total Desired Torque Calculation Locations according to Hybrid Drive System Architecture**

The vehicle total desired torque according to architecture is calculated as Equation (3) ~ (9). We considered the efficiency of the transmission in a real simulation, but not present in this paper to simplify equation representation. In the equation below,  $T_{e0}$  is drive resistance torque of the engine,  $T_{wp}$  is load torque of the mechanical auxiliary load,  $T_{m0,i}$  ( $i=2$  for P2, 3 for P3, 0D3 for P0D+P3, etc.) is the drive resistance torque of the motor, and  $\gamma_{fd}$  is the gear ratio of the final drive gear. Here,  $T_{e0}$  and  $T_{wp}$  are calculated at the transmission input shaft. Therefore, for the architecture which calculates vehicle total desired

torque at the transmission output shaft, we should calculate these values considering the transmission gear ratio. And since  $T_{m0,i}$  is calculated at motor shaft, we should calculate the drive resistance torque of the motor considering the transmission gear ratio or motor location when calculating vehicle total desired torque. In the equation below,  $T_{e0\_diff}$ ,  $T_{m0,i\_diff}$ ,  $T_{wp\_diff}$  are drive resistance torque of the engine and motor considering the transmission gear ratio, mechanical auxiliary load torque considering the transmission gear ratio respectively.

1. P2

$$T_{tot,2} = \begin{cases} T_{e0} + T_{wp} + T_{m0,2} + \frac{T_v}{\gamma_{TM}\gamma_{fd}} & (u_1 \neq 1) \\ T_{m0,2} + \frac{T_v}{\gamma_{TM}\gamma_{fd}} & (u_1 = 1) \end{cases} \quad (3)$$

2. P3, P4 ( $k = 3, 4$ )

$$T_{tot,k} = \begin{cases} T_{e0\_diff} + T_{wp\_diff} + T_{m0,k} + \frac{T_v}{\gamma_{fd}} & (u_1 \neq 1) \\ T_{m0,k} + \frac{T_v}{\gamma_{fd}} & (u_1 = 1) \end{cases} \quad (4)$$

3. P0D+P2

$$T_{tot,0D2} = \begin{cases} T_{e0} + T_{wp} + T_{m0,2} + T_{m0,0D}\gamma_{ply} + \frac{T_v}{\gamma_{TM}\gamma_{fd}} & \{(u_1 \neq 1) \& (u_4 \neq 1)\} \\ T_{e0} + T_{m0,1} + \frac{T_v}{\gamma_{TM}\gamma_{fd}} & \{(u_1 \neq 1) \& (u_4 = 1)\} \\ T_{m0,1} + \frac{T_v}{\gamma_{TM}\gamma_{fd}} & \{(u_1 = 1)\} \end{cases} \quad (5)$$

4. P0D+P3, P0D+P4 ( $k = 3, 4$ )

$$T_{tot,0Dk} = \begin{cases} T_{e0\_diff} + T_{wp\_diff} + T_{m0,k} + T_{m0,0D\_diff} + \frac{T_v}{\gamma_{fd}} & \{(u_1 \neq 1) \& (u_4 \neq 1)\} \\ T_{e0\_diff} + T_{m0,k} + \frac{T_v}{\gamma_{fd}} & \{(u_1 \neq 1) \& (u_4 = 1)\} \\ T_{m0,k} + \frac{T_v}{\gamma_{fd}} & \{(u_1 = 1)\} \end{cases}$$

(6)

5. P1+P2

$$T_{tot,12} = \begin{cases} T_{e0} + T_{wp} + T_{m0,1} + T_{m0,2} + \frac{T_v}{\gamma_{TM}\gamma_{fd}} & (u_1 \neq 1) \\ T_{m0,1} + \frac{T_v}{\gamma_{TM}\gamma_{fd}} & (u_1 = 1) \end{cases} \quad (7)$$

6. P1+P3, P1+P4 ( $k = 3, 4$ )

$$T_{tot,1k} = \begin{cases} T_{e0\_diff} + T_{wp\_diff} + T_{m0,k} + T_{m0,1\_diff} + \frac{T_v}{\gamma_{fd}} & (u_1 \neq 1) \\ T_{m0,k} + \frac{T_v}{\gamma_{fd}} & (u_1 = 1) \end{cases} \quad (8)$$

7. P2+P4

$$T_{tot,24} = \begin{cases} T_{e0\_diff} + T_{wp\_diff} + T_{m0,4} + T_{m0,2\_diff} + \frac{T_v}{\gamma_{fd}} & (u_1 + u_5 \neq 1) \\ T_{m0,4} + T_{m0,2} + \frac{T_v}{\gamma_{fd}} & (u_1 + u_5 = 1) \end{cases} \quad (9)$$

### 3.3.2. Motor torque determination by $u_1$ (First motor)

Table 6 shows the motor of which torque is determined by control input  $u_1$ , according to the architecture, and we let say this motor as the first motor from now on. The torque of the motor is calculated as Equation (10). In the Equation (10),  $T_{m,i}$  is the torque of the motor of which torque is determined by  $u_1$  for each architecture, and  $T_{tot,k}$  is the vehicle total desired torque for each architecture.

**Table 6: The Motor of which Torque is determined by Control Input  $u_1$**

Architecture		Architecture	
P2	P2	P0D+P4	P4
P3	P3	P1+P2	P2
P4	P4	P1+P3	P3
P0D+P2	P2	P1+P4	P4
P0D+P3	P3	P2+P4	P4

$$T_{m,i} = u_1 T_{tot,k} \quad (i = 2, 3, 4, k = 2, 3, 4, 0D2, 0D3, \dots) \quad (10)$$

### 3.3.3. Motor torque determination by $u_5$ (Second motor)

Table 7 shows the motor of which torque is determined by control input  $u_5$ , according to the architecture, and we let say this motor as the second motor from now on.

**Table 7: The Motor of which Torque is determined by Control Input  $u_5$**

Architecture		Architecture	
P0D+P2	P0D	P1+P2	P1
P0D+P3		P1+P3	
P0D+P4		P1+P4	
	P2+P4		

If the case of  $u_1 = 1$ , since the vehicle is propelled by the first motor only, the second motor doesn't generate any torque. Therefore, the second motor torque is determined differently by  $u_1$ . And in the case of P0D motor, the torque of the motor is differed by decoupler state. With consideration of these characteristics, the motor torque is determined like Equation (11) ~ (16), according to the architecture. In Equation (13),  $C_{eff}$  is the efficiency of delivered driving power, and  $\eta_{trans}$  has the value between 0 and 1. This is the parameter for reflecting power distribution characteristic when motors are located at both front and rear wheel. For example, when the motors of the front and rear wheel all propel the vehicle or all brake the vehicle, each drive power is delivered to ground directly. But when the motor of front wheel propels the vehicle and the motor of rear wheel generate power using front wheel power, the front wheel power is delivered rear wheel motor through the ground. So, in that case, we should consider the efficiency of the delivered drive power. For reflecting these characteristics, we use  $C_{eff}$  when architecture has a P4 motor.

1. P0D+P2

$$T_{m,0D} = \begin{cases} u_5 \frac{T_{tot,0D2}}{\gamma_{ply}} & \{(u_4 \neq 1) \& (u_1 \neq 1)\} \\ 0 & \{(u_4 \neq 1) \& (u_1 = 1)\} \\ T_{m0m0D} + \frac{T_{wp}}{\gamma_{ply}} & \{(u_4 = 1)\} \end{cases} \quad (11)$$

2. P0D+P3

$$T_{m,0D} = \begin{cases} u_5 \frac{T_{tot,0D3}}{\gamma_{TM} \gamma_{ply}} & \{(u_4 \neq 1) \& (u_1 \neq 1)\} \\ 0 & \{(u_4 \neq 1) \& (u_1 = 1)\} \\ T_{m0,0D} + \frac{T_{wp}}{\gamma_{ply}} & \{(u_4 = 1)\} \end{cases} \quad (12)$$

### 3. POD+P4

$$T_{tot,f,0D4} = T_{tot,0D4} - C_{eff} T_{m,4}$$

$$C_{eff} = \begin{cases} 1/\eta_{trans} & \{(T_{tot,0D4} \geq 0) \& (u_1 T_{m,4} \leq 0)\} \\ I & (otherwise) \end{cases}$$

$$T_{m,0D} = \begin{cases} u_5 \frac{T_{tot,f,0D4}}{\gamma_{TM} \gamma_{ply}} & \{(u_4 \neq 1) \& (u_1 \neq 1)\} \\ 0 & \{(u_4 \neq 1) \& (u_1 = 1)\} \\ T_{m0,0D} + \frac{T_{wp}}{\gamma_{ply}} & \{(u_4 = 1)\} \end{cases} \quad (13)$$

### 4. P1+P2

$$T_{m,1} = \begin{cases} u_5 T_{tot,12} & (u_1 \neq 1) \\ 0 & (u_1 = 1) \end{cases} \quad (14)$$

### 5. P1+P3

$$T_{m,1} = \begin{cases} u_5 \frac{T_{tot,13}}{\gamma_{TM}} & (u_1 \neq 1) \\ 0 & (u_1 = 1) \end{cases} \quad (15)$$

### 6. P1+P4, P2+P4

$$T_{m,1} = \begin{cases} u_5 \frac{T_{tot,f,14}}{\gamma_{TM}} & (u_1 \neq 1) \\ 0 & (u_1 = 1) \end{cases} \quad (16)$$

### 3.3.4. Cost

The `dpm.m` function sum the all cost per step to determine the optimal path. In this paper, the cost is defined by performance index differently.

The cost for fuel economy and additional performance index, electric auxiliary load assist ability is fuel consumption per step time like Equation (17). Therefore, The *DP* for fuel economy and electric auxiliary assist ability will find the optimal path which minimizes fuel consumption.

The cost for drive power reserve is like Equation (18). In the equation,  $\Delta m_{fuel}$  is fuel consumption per step time,  $k_{pwr}$  is the coefficient for drive power reserve,  $P_{e,max}, P_e$  are the engine maximum power and current power respectively,  $\omega_e, \omega_{e-SC}$  are the speed of the engine and 48V electric supercharger respectively,  $H_{LHV}$  is a low-heating value of fuel,  $T_s$  is step time. And we can see that the second term of Equation (18) has the same unit with fuel consumption. By this term, the engine drive power reserve (The engine maximum power – current power) became larger, the cost became smaller. So, The *DP* for drive power reserve will find the optimal path which maximizes drive power reserve and minimizes fuel consumption.

$$J = \Delta m_{fuel} \quad (17)$$

$$J = \Delta m_{fuel} - k_{pwr} \frac{P_{e,max}(\omega_e, \omega_{e-SC}) - P_e}{H_{LHV}} T_s \quad (18)$$

## 4. DYNAMIC PROGRAMMING RESULT

### 4.1. Test scenario

In order to compare performance for each architecture, we carry out *DP* simulation for FTP-75 which is one of the driving cycles that used for evaluating fuel economy of a hybrid electric vehicle generally. The speed profile reference of a vehicle is like Figure 4.

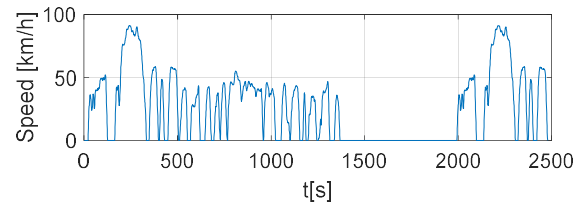


Figure 4: The Speed Profile of FTP-75 Cycle

### 4.2. Performance index

In this paper, we evaluate hybrid drive system architecture through fuel economy, electric auxiliary load assist ability, and drive power reserve. The index for evaluating each performance is calculated like below respectively.

#### 4.2.1. Fuel economy

We calculate fuel economy like Equation (19) that calculate fuel economy by the total fuel consumption versus total travel distance of the vehicle. In this case, the cost of Model function.m is Equation (17). In the Equation (19), *FE* is fuel economy of the vehicle,

$Dist_{tot}$  is total travel distance of the vehicle when driving FTP-75 cycle,  $F_{base}$  is total fuel consumption when we use cost as Equation (17).

$$FE = \frac{Dist_{tot}}{\sum \Delta m_{fuel}}, F_{base} = \sum \Delta m_{fuel} \quad (19)$$

#### 4.2.2. Electric auxiliary load assist ability performance index

For the case of electric auxiliary load assist ability, the cost of the Model function.m is Equation (17) as the case of fuel economy also. We evaluate the electric auxiliary load assist ability by fuel consumption difference between when an additional electric auxiliary load is applied and when is not applied. If the difference is not large, we can say that the architecture has high electric auxiliary load assist ability because it has a low reduction of fuel economy by an additional electric auxiliary load.

In order to compare performance according to an additional electric auxiliary load size, we apply two kinds of additional loads, 300[W] and 1000[W]. The electric auxiliary load assist ability is defined as Equation (20). In Equation (20),  $F_{FE,base}$  is the fuel consumption when an additional electric auxiliary load is not applied,  $F_{FE,accelec}$  is the fuel consumption when an additional electric auxiliary load,  $P_{elec,add}$ , is applied by 300[W] or 1000[W].

$$\begin{aligned} F_{elec,acc} &= F_{FE,accelec} - F_{FE,base} \\ F_{FE,base} &= \sum \Delta m_{fuel} (@P_{elec,add} = 0) \\ F_{FE,accelec} &= \sum \Delta m_{fuel} (@P_{elec,add} = 300 \text{ or } 1000) \end{aligned} \quad (20)$$

#### 4.2.3. Drive power reserve performance index

We evaluate the performance of the drive power reserve as the total summation of drive power reserve per step time when we set the cost of Model function.m as Equation (18). In other words, the drive power reserve performance  $F_{pwr,rsv}$  is defined as Equation (21).

$$F_{pwr,rsv} = \sum \frac{P_{e,max}(\omega_e, \omega_{e-SC}) - P_e}{H_{LHV}} T_s \quad (21)$$

#### 4.2.4. Comprehensive performance index

We defined the performance of electric auxiliary load assist ability and drive power reserve as Equation (20), (21). We defined each performance index as the concept of fuel consumption, and the reason for this is to solve the scaling problem when calculating the comprehensive performance index. The comprehensive performance index ( $F_{total}$ ) that integrates all performance index which is described earlier is Equation (22). In Equation (22),  $\alpha_0$ ,  $\alpha_1$ , and  $\alpha_2$  are the weight of each performance index respectively, and a user can adjust the weight when deriving optimal hybrid system architecture, according to what performance is more important. For example, If a user wants the optimal architecture which has higher electric auxiliary load assist ability than fuel economy and the drive power reserve, the user can set the weight as  $\alpha_0 = 0.1$ ,  $\alpha_1 = 1$ ,  $\alpha_2 = 0.1$ . Each weight has a positive value.

$$F_{total} = \alpha_0 F_{base} + \alpha_1 F_{elec,acc} - \alpha_2 F_{pwr,rsv} \quad (22)$$

#### 4.3. Comparison of fuel economy

The fuel economy results for each architecture obtained by DP simulation (FTP-75) is like Figure 5. In this case, we set the cost of Model function.m as Equation (17). We can see P2 architecture have the best fuel economy. The reason for this may be that the motor of P2 architecture can operate at a higher efficiency operating point than other architecture by optimizing the gear stage. And for all architectures, we can see that they have higher fuel economy when a 48V electric supercharger is applied. Therefore, we can conclude that the optimal architecture for fuel economy is P2 with e-SC (48V electric supercharger) architecture.

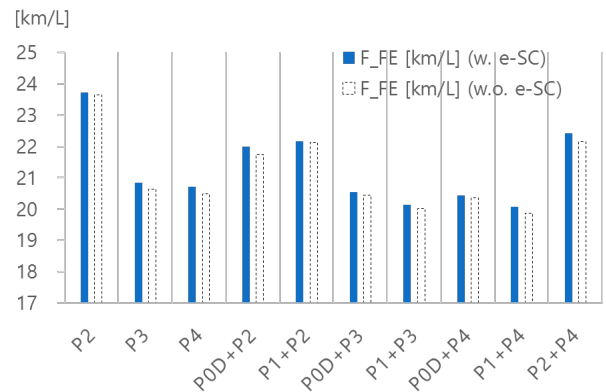


Figure 5: Comparison of FE

#### 4.4. Comparison of electric auxiliary load assist ability

The electric auxiliary load assist ability for each architecture obtained by *DP* simulation (FTP-75) is like Figure 6, 7. In this case, we set the cost of Model function.m as Equation (17) and apply additional electric auxiliary load. Figure 6 and 7 are the case when an additional electric auxiliary load is 300[W] and 1000[W] respectively. The electric auxiliary load assist ability performance index has a low value when the electric auxiliary load assist ability is high. For both cases that additional electric auxiliary loads are 300[W] and 1000[W] respectively, we can see that the P0D+P2 with e-SC architecture has the best electric auxiliary load assist ability. Therefore, we can conclude that the optimal architecture for the electric auxiliary load assist ability is P0D+P2 with e-SC architecture.

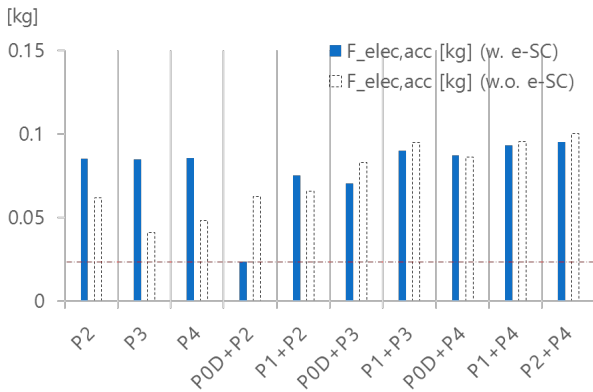


Figure 6: Comparison of  $F_{elec,acc}$  ( $P_{elec,add} = 300$ )

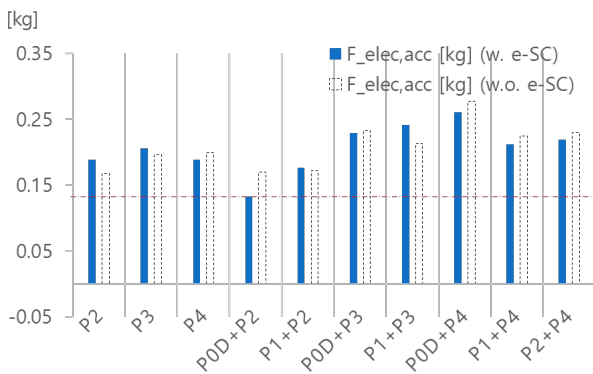


Figure 7: Comparison of  $F_{elec,acc}$  ( $P_{elec,add} = 1000$ )

#### 4.5. Comparison of drive power reserve

The drive power reserve for each architecture obtained by *DP* simulation (FTP-75) is like Figure 8. In this case, we set the cost of Model function.m as Equation (18). The drive power reserve performance index has a high value when the drive power reserve is high. So, we can see that the P0D+P2 without e-SC architecture has the

best drive power reserve. Therefore, we can conclude that the optimal architecture for the drive power reserve is P0D+P2 without e-SC architecture.

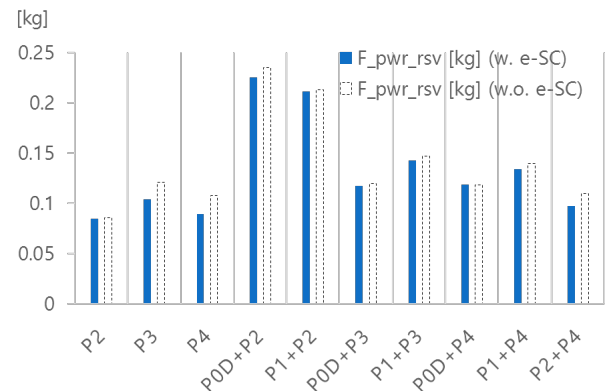


Figure 8: Comparison of  $F_{pwr,rsv}$

#### 4.6. Comparison of Comprehensive Performance Index

The comprehensive performance index is differed by weight value,  $\alpha_0, \alpha_1, \alpha_2$ . In this paper, we show one examples by setting  $\alpha_0, \alpha_1, \alpha_2$  to 1 all. In other words, the optimal architecture derived from these weight values will be the architecture that has proper fuel economy, electric auxiliary load assist ability and drive power reserve. We calculate the comprehensive performance index for each architecture using performance indices which are calculated in previous sections, and the results are like Figure 9, 10. For both cases of additional electric auxiliary load are 300[W] and 1000[W] respectively, we can see that the P0D+P2 without e-SC architecture has the lowest comprehensive performance index. Therefore, we can conclude that the optimal architecture for the comprehensive performance index is P0D+P2 without e-SC architecture.

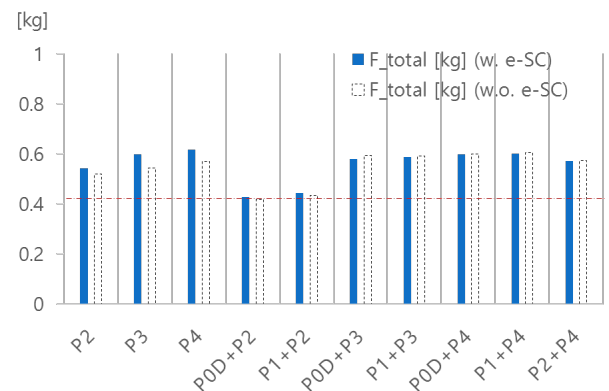


Figure 9: Comparison of  $F_{total}$  ( $P_{elec,add} = 300$ )

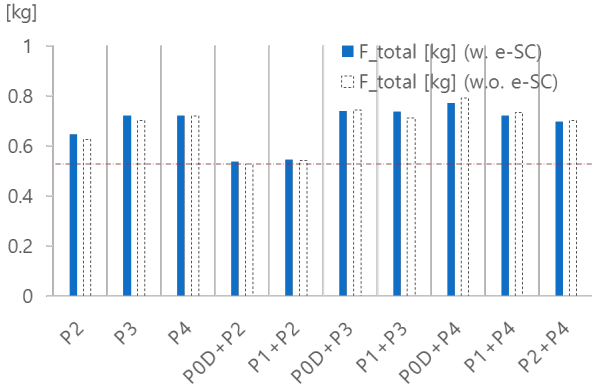


Figure 10: Comparison of  $F_{total}$  ( $P_{elec,add} = 1000$ )

#### 4.7. Ranking by Each Performance Index

Table 8 and 9 are the ranking of the performance indices which are calculated in previous sections. The ranking is low when performance is high. In other words,  $FE$ ,  $F_{pwr,rsv}$  are ordered in which the performance indices are high, and  $P_{elec,add}$  are ordered in which the performance indices are low.

In the case of fuel economy, we can see that the architectures having the P2 motor tend to have a high fuel economy. And In the case of the drive power reserve, we can see that the architecture having the motor connected directly to the engine crankshaft (POD, P1) tend to have a high drive power reserve. In the case of the electric auxiliary load assist ability, we can't find a clear trend when an additional electric auxiliary load is 300[W]. But when an additional electric auxiliary load is 1000[W], we can see that the architecture having both P2 motor and the motor connected directly to the engine crankshaft tend to have a high electric auxiliary load assist ability.

Therefore, taking above analysis together, we can conclude that we should select the P2 architecture when fuel economy is the most important, and select the architecture having crankshaft direct connection motor and P2 motor when electric auxiliary load assist ability or drive power reserve is most important.

Table 8: Ranking by  $FE$  and  $F_{pwr,rsv}$

Rank	$FE$		$F_{pwr,rsv}$	
	Architecture	48V e-SC	Architecture	48V e-SC
1	P2	O	P0D+P2	-
2	P2	-	P0D+P2	O
3	P2+P4	O	P1+P2	-
4	P1+P2	O	P1+P2	O
5	P2+P4	-	P1+P3	-
6	P1+P2	-	P1+P3	O
7	P0D+P2	O	P1+P4	-
8	P0D+P2	-	P1+P4	O
9	P3	O	P3	-
10	P4	O	P0D+P3	-
11	P3	-	P0D+P4	-
12	P0D+P3	O	P0D+P4	O
13	P4	-	P0D+P3	O
14	P0D+P4	O	P2+P4	-
15	P0D+P3	-	P4	-
16	P0D+P4	-	P3	O
17	P1+P3	O	P2+P4	O
18	P1+P4	O	P4	O
19	P1+P3	-	P2	-
20	P1+P4	-	P2	O

Table 9: Ranking by  $P_{elec,add}$

Rank	$F_{elec,acc}$ ( $P_{elec,add} = 300$ )		$F_{elec,acc}$ ( $P_{elec,add} = 1000$ )	
	Architecture	48V e-SC	Architecture	48V e-SC
1	P0D+P2	O	P0D+P2	O
2	P3	-	P2	-
3	P4	-	P0D+P2	-
4	P2	-	P1+P2	-
5	P0D+P2	-	P1+P2	O
6	P1+P2	-	P2	O
7	P0D+P3	O	P4	O
8	P1+P2	O	P3	-
9	P0D+P3	-	P4	-
10	P3	O	P3	O
11	P2	O	P1+P4	O
12	P4	O	P1+P3	-
13	P0D+P4	-	P2+P4	O
14	P0D+P4	O	P1+P4	-
15	P1+P3	O	P0D+P3	O
16	P1+P4	O	P2+P4	-
17	P1+P3	-	P0D+P3	-
18	P2+P4	O	P1+P3	O
19	P1+P4	-	P0D+P4	O
20	P2+P4	-	P0D+P4	-

## 5. CONCLUSION

In this paper, we selected exploration target 48V hybrid drive architecture by exploring possible 48V hybrid drive system manually and compared the performance of each architecture through *DP* simulation. When comparing the performance of the hybrid system, we used not only fuel economy but also electric auxiliary load assist ability and drive power reserve. Here, we developed performance indices for electric auxiliary load assist ability and drive power reserve in order to compare performance. And the performance indices have a unit of fuel consumption in order to solve the problem scaling when calculating comprehensive performance index. As results, we found that P2 is the optimal architecture for fuel economy, and the architecture having crankshaft direct connection motor (POD, P1) and P2 motor is the optimal architecture for electric auxiliary load assist ability or drive power reserve.

We considered an engine only when calculating drive power reserve performance index. But a hybrid electric vehicle has not only an engine but also a motor for driving. Therefore, in future work, if we consider a drive power reserve of an engine and a motor together, the drive power reserve performance is expected to be evaluated more accurately.

## ACKNOWLEDGMENTS

This work was supported by the Industrial Strategic Technology Development Program (10076437, Development of hybrid drive topology exploration and control technology for fuel economy optimization of 48V mild HEVs) funded By the Ministry of Trade, Industry & Energy(MOTIE, Korea).

## REFERENCES

- Andreas Baumgardt, Dieter Gerling, 2015a. 48V Recuperation Storage Based on Supercaps for Automotive Application, EVS28 International Electric Vehicle Symposium and Exhibition, May 3-6, KINTEX (Korea).
- Andreas Baumgardt, Dieter Gerling, 2015b. 48V Recuperation Storage Including Stabilizing 12V Tap for HEVs, 2015 IEEE Transportation Electrification Conference and Expo (ITEC), June 14-17, Dearborn (Michigan, USA).
- Anthony Rick, Brain Sisk, 2015. A Simulation Based Analysis of 12V and 48V Microhybrid Systems Across Vehicle Segments and Drive Cycle, SAE 2015 World Congress & Exhibition, April 21-23. Detroit (Michigan, USA).
- Dr. Ing. Olivier COPPIN, 2016. Valeo Presentation – From 12 plus 12V to 48V. Available from: <https://48v-vehicles.iqpc.de/downloads/valeo-presentation-from-12-plus-12v-to-48v> [accessed 5 March 2019]
- Ji Y., Park J, Lee H., 2018. A study on operating characteristics of a 48V electric supercharger and P0 configuration motor for fuel economy improvement. MAS 2018, September 17, 39-47.
- Junyong Park, Taeho Park, Hyeongcheol Lee, 2017. An optimization of power distribution considering supercharging characteristic for electric supercharger applied 48V mild hybrid vehicle, KSAE 2017 Annual Autumn Conference & Exhibition, pp.1328-1333. November 15-18, Yeosu (Jeollanam-do, South Korea).
- Kapadia J., Kok D., Jennings M., Kuang M., Masterson B., Isaacs R., Dona A., Wagner C., and Gee T., 2017. Powersplit or Parallel - Selecting the Right Hybrid Architecture. SAE International Journal of Alternative Powertrains, 6.
- Malte Kuypers, 2014. Application of 48 Volt for Mild Hybrid Vehicles and High Power Load, SAE 2014 World Congress & Exhibition, April 1, Detroit (Michigan, USA).
- Mark Schudeleit, Christian Sieg, Ferit Küçükay, 2015. The Potential of 48V HEV in Real Driving, International Scholarly and Scientific Research & Innovation Vol: 9 No: 10, 1719-1728.
- Olle Sundstrom, Lino Guzzella, 2009. A Generic Dynamic Programming Matlab Function, 18<sup>th</sup> IEEE International Conference on Control Applications Part of 2009 IEEE Multi-conference on Systems and Control Saint Petersburg, July 8-10, St. Petersburg (Russia).
- Ran Bao, Victor Avila, James Baxter, 2017. Effect of 48V Mild Hybrid System Layout on Powertrain System Efficiency and Its Potential of Fuel Economy Improvement, WCX™ 17: SAE World Congress Experience, April 4-6, Detroit (Michigan, USA).
- Thomas Eckenfels, Florian Kolb, Steffen Lehmann, Waldemar Neugebauer, Manel Calero, 2018. 48V Hybridization, A Smart Upgrade for the Powertrain. Available from: <http://schaeffler-events.com/symposium/lecture/h3/index.html> [accessed 6 July 2018]
- Zifan Liu, Andrej Ivanco, and Zoran S. Filipi, 2016. Impact of Real-World Driving and Driver Aggressiveness on Fuel Consumption of 48V Mild Hybrid Vehicle, SAE International, April 5, 249-258.